catalysts

MDPI

Article

Levulinic Acid Production from Delignified Rice Husk Waste over Manganese Catalysts: Heterogeneous Versus Homogeneous

Arnia Putri Pratama, Dyah Utami Cahyaning Rahayu and Yuni Krisyuningsih Krisnandi *

Department of Chemistry, Faculty of Mathematics and Natural Sciences, Universitas Indonesia, Depok 16424, Indonesia; arnia.putri@sci.ui.ac.id (A.P.P.); dyahutamicr@sci.ui.ac.id (D.U.C.R.)

* Correspondence: yuni.krisnandi@sci.ui.ac.id; Tel.: +62-812-1856-7060

Received: 20 February 2020; Accepted: 12 March 2020; Published: 14 March 2020

Abstract: Delignified rice husk waste (25.66% (wt) cellulose) was converted to levulinic acid using three types of manganese catalysts, i.e., the Mn_3O_4/hierarchical ZSM-5 zeolite and Mn_3O_4 heterogenous catalysts, as well as Mn(II) ion homogeneous counterpart. The hierarchical ZSM-5 zeolite was prepared using the double template method and modified with Mn_3O_4 through wet-impregnation method. The structure and physicochemical properties of the catalyst materials were determined using several solid-state characterization techniques. The reaction was conducted in a 200 mL-three neck-round bottom flask at 100 °C and 130 °C for a certain reaction time in the presence of 10% (v/v) phosphoric acid and 2% (v/v) H_2O_2 aqueous solution, and the product was analyzed using HPLC. In general, 5-hydroxymethyl furfural (5-HMF) as the intermediate product was produced after 2 h and decreased after 4 h reaction time. To conclude, the Mn_3O_4/hierarchical ZSM-5 heterogenous catalyst gave the highest yield (wt %) of levulinic acid (39.75% and 27.60%, respectively) as the main product, after 8 h reaction time.

Keywords: levulinic acid; manganese catalysts; hierarchical ZSM-5; lignocellulose conversion

1. Introduction

Levulinic acid (4-oxopentanoic acid) is an important compound used as a platform chemical in alternative energy production, such as the production of γ-valerolactone (GVL), 5-bromolevulinic acid, valeric acid, 2-methyl-THF, and methyl pyrrolidone [1]. It is also used as a renewable source for the production of polymers such as its derivative, GVL, which is used as a basis for precursor formation of polymers [2]. Kon et al. reported reacting levulinic acid with valeric acid and valeric biofuels via selective hydrogenation using a Pt/HMFI zeolite catalyst [3]. One of the important industrial heterogeneous catalysts used as support is micropores zeolite (>2 nm pore diameter). It is well-known that zeolite has thermal and chemical stability, as well as catalytic and adsorption activity [4]. However the micropores has limited the application of zeolite in conversion or adsorption of larger substrates. Therefore, some attempts have been reported to improve overcome this limitation including preparing hierarchical zeolite [5]. In contrast to conventional zeolites, hierarchical zeolites consist of both micropores (where the active sites located) and mesopores facilitating diffusion of reactants and products [6].

Preparation of hierarchical ZSM-5 and other zeolites structure using secondary template have been reported, such as hierarchical mesoporous Beta and ZSM-5 [7], also mesoporous FAU type zeolite [8]. ZSM-5, one type of zeolites has long been used as catalyst in the fine-chemical and petrochemicals industry for catalytic reactions involving cracking, isomerization, alkylation, acylation, purification for water adsorbing systems [9], and having active sites with diverse strength become the main attractions

related to their application [10]. Hierarchical ZSM-5 zeolites used for partial oxidation of methane to methanol [11], catalytic hydrogenation of carbon dioxide [12], catalytic pyrolysis of biomass to aromatic hydrocarbons [13].

In many industries, the production of levulinic acid is relatively low because of the high cost of its synthetic raw materials. Hence, the importance of biomass raw materials, which are cheap and easy to make, cannot be overemphasized [14]. Indonesia is the third largest rice producer in the world, after China and India. However, the country has yet to attain optimal utilization of rice husk. To overcome the above limitations and make proper use of the abundant raw materials, rice husks can be used as organic (biomass) substitutes for synthetic raw materials in the production of levulinic acid, using the cellulose contained in biomass. It is necessary to optimize the delignification pre-treatment to obtain optimum amount of cellulose from lignocellulosic biomass. There are several methods of chemical delignification such as ozonolysis, oxidative delignification, acid and alkaline hydrolysis. The alkali pretreatment using NaOH is the most common method applied, where the NaOH concentration depends on the content of lignin in the plants. In example, diluted NaOH solution is effective to reduce lignin content (wt %) from 24–55% to 20% (wt) in hardwood [15]. In our previous work, pretreatment of mahogany wood with NaOH 10% (v/v) decreased the lignin content from 51.03 to 15.58% (wt) [16], whereas when applied to rice husk, the lignin content was decreased from 35.64 to 18.42% (wt) [17]. NaOH showed to be the best delignification agent because the obtained cellulose is more amorphous, compared to NaOCl giving more crystalline cellulose [16].

Chen et al. [17] studied the degradation of pure cotton cellulose into 5-(hydroxymethyl)furfural (5-HMF) and levulinic acid, using Mn/ZSM-5 agregate as catalyst through Fenton-like reaction. The degradation process investigated the use of Mn/ZSM-5 as catalyst for the degradation of pure cotton cellulose under phosphoric acid media and hydrogen peroxide, to yield 5-HMF as a main product and levulinic acid as a by-product. In other work, HCl has been used as a homogeneous catalyst while ZSM-5, β-zeolite, Y-zeolite were used as heterogeneous catalysts transform glucose into levulinic acid and 5-HMF [18]. In our previous study, Krisnandi et al. [17] used hierarchical MnOx/ZSM-5 as heterogeneous catalyst and Mn^{2+} ions as homogeneous catalyst in conversion of delignified rice husk to levulinic acid. The conversion recorded a highest percentage yield (wt %) for levulinic acid (15.83%) at 100 °C, reaction time of 8 h, and in phosphoric acid media containing H_2O_2. It showed the stability of the heterogeneous catalysts after the reaction.

In order to obtain more information the role of manganese oxide and hierarchical ZSM-5 in Mn3O4/hierarchical ZSM-5 catalysts, conversion with manganese oxide Mn_3O_4 (as heterogeneous catalyst) was also carried out as addition to experiments reported in [17]. Furthermore, identification of intermediate compound (HMF) and side product (formic acid) were also carried out. Therefore, mechanism in conversion cellulose to levulininc acid can be confirmed. To the best of the author knowledge, this is one among not many articles reporting the utilization of raw biomass as cellulose sources which contributed to the development of value-added chemical such as levulinic acid.

2. Results

2.1. Catalyst Characterization

XRD analysis was conducted to confirm the structure of the as-synthesized ZSM-5 zeolite. Its diffraction pattern (Figure 1) has typical peaks similar to those observed in the pattern of standard ZSM-5, in which there are two sharp peaks between 2θ = 7–10° and three peaks between 2θ = 22–25° [19].

The powder XRD pattern of the Mn_3O_4/hierarchical ZSM-5 zeolite (Figure 1b) show additional peaks which include, two sharp peaks between 2θ = 30–35°, and three peaks between 2θ = 35–40° [20]. According to JCPDS: 24-0734, peaks belong to Mn3O4 crystals. These results indicate the successful preparation of hierarchical Mn_3O_4/ZSM-5 samples. On the other hand, a sharp peak between 2θ = 15–20° is also observed at XRD pattern of as-prepared Mn3O4 (Figure 1c), according to JCPDS: 44-0141, the peak belongs to MnO_2 [21].

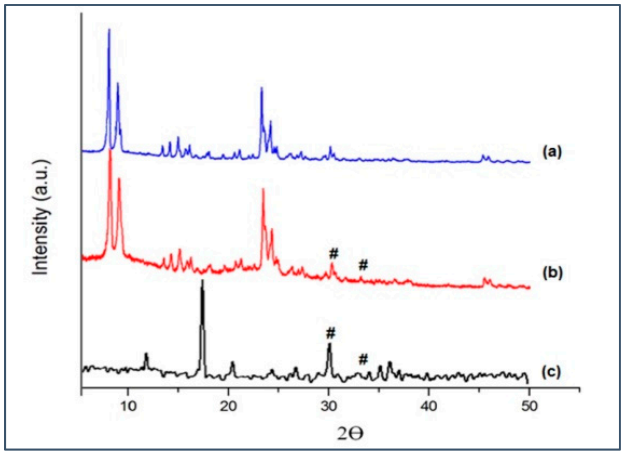

Figure 1. X-ray diffraction patterns of the (**a**) ZSM-5 and (**b**) Mn_3O_4/ZSM-5 (**c**) Mn_3O_4 (# Mn_3O_4 peaks JCPDS: 24–0734).

FTIR analysis of ZSM-5 zeolites and manganese oxide-modified counterpart is summarized in Figure 2. The infrared spectra of hierarchical Mn_3O_4/ZSM-5 zeolite (Figure 2b) was compared to that of hierarchical ZSM-5 zeolite (Figure 2c) and Mn_3O_4 (Figure 2a). The figures show that all the peaks observed in the hierarchical ZSM-5 zeolite were also observed in the Mn_3O_4/hierarchical ZSM-5 zeolite. However, there is a difference in the intensity of the broad band located at 3500–3000 cm^{-1}, which is a typical absorption band assigned to the stretching vibration of water-hydrogen bonded silanol group (ν-Si–OH) or internal silanol groups [22]. The intensity of the silanol band in Mn_3O_4/ZSM-5 decreased, suggesting that the Mn-oxide species were located on top of the silanol groups, thus they interacted with the –OH, thereby leading to a decrease in the water content of the water-hydrogen bonded –Si-OH group. In addition, Figure 2 shows the presence of Mn_3O_4 where the FTIR spectra indicate two characteristic emission bands located around 613 and 509 cm^{-1}, a typical absorption band coupling between Mn−O stretching at the finger print area [23]. In addition, there were more than two absorption band peaks around 615 and 513 cm^{-1}, which can be attributed to the coupling modes between the Mn–O stretching, while the band around 429 cm^{-1} can be assigned as a band-stretching mode [24].

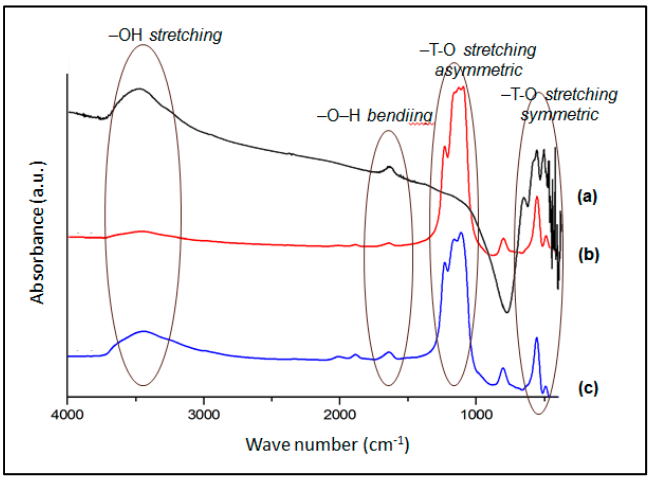

Figure 2. Infrared spectra of catalyst samples: (**a**) Mn_3O_4; (**b**) hierarchical ZSM-5; (**c**) Mn_3O_4/hierarchical ZSM-5.

AAS measurement for the Mn-oxide ZSM-5 indicates that the weight percent loading of Mn into the ZSM-5 structure was 1.91% (wt %), which is close to the expected value of 2.0%. It can also be seen that the insertion of Mn_3O_4 into the extra zeolite framework did not cause significant change

to its XRD pattern. This indicates that the structure and crystallinity of the ZSM-5 zeolite were not destroyed during the Mn impregnation process.

Scanning electron microscopy (SEM) characterization provided morphology information of the hierarchical ZSM-5 zeolite. Figure 3 clearly shows that the as-synthesized ZSM-5 zeolite had hexagonal structure and a coffin-like shape [25]. ZSM-5 zeolite synthesized using TPAOH template to form MFI framework has coffin-like morphology and has hexagonal crystal geometry [7]. However, the mesoporosity of the surface is not clearly visible, as reported by Wang et al. [7]. Therefore, it is necessary to perform surface area analysis to identify the ZSM-5 as a porous material.

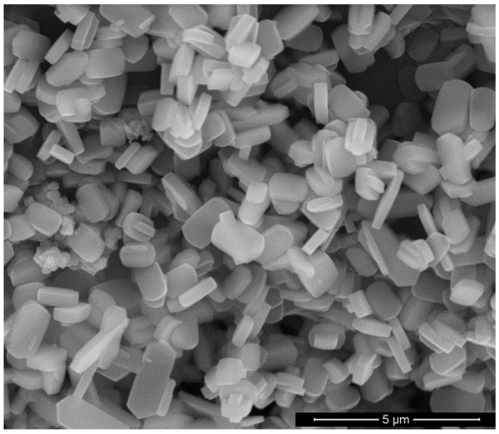

Figure 3. Images of scanning electron microscopy (SEM) characterization of Hierarchical ZSM-5 Zeolite, magnification 20,000 ×.

Transmission Electron Microscope (TEM) measurement (Figure 4) of the hierarchical ZSM-5 zeolite and its modification with Mn_3O_4 indicates that the crystal morphology of the catalyst is not damaged after modification. There are some bright oval shapes with diameter sizes of 2.5–12 nm (Figure 4a) that justify the presence of mesoporosity within the structure of hierarchical ZSM-5. This corresponds with the SEM images and SAA data. In the image of Mn_3O_4-modified ZSM-5 shown in Figure 4b, dark deposits were observed on the surface of hierarchical ZSM-5, which could be attributed to the presence of Mn_3O_4 cluster aggregation with diameter size of 6.8–20 nm.

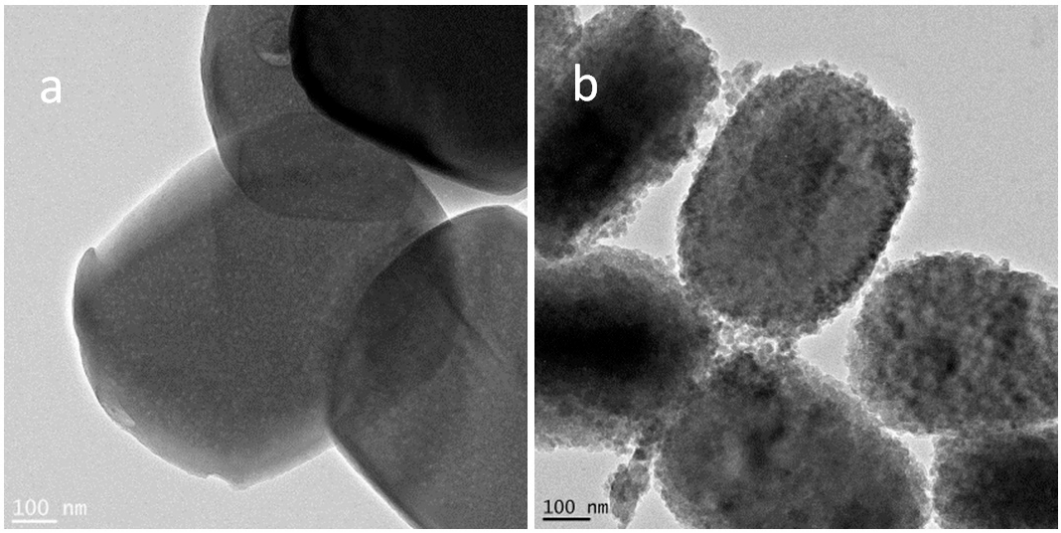

Figure 4. TEM image characterization of (**a**) hierarchical ZSM-5 zeolite and (**b**) Mn_3O_4/hierarchical ZSM-5 zeolite.

The analysis of the surface area and pore size were carried out using Brunauer–Emmett–Teller (BET) and Barrett–Joyner–Halenda (BJH) desorption methods, respectively. The results showed that the surface area of the as-synthesized hierarchical ZSM-5 zeolite was 348.6 m^2/g. This property is important, because the greater the surface area, the easier it is to disperse metal oxides as active sites on the support surface [26]. Furthermore, Figure 5 shows the characteristic isotherm curves (type IV), which indicates a mesoporous structure. PDDA-Cl (polidialydimethyl ammonium chloride) aims to build this hierarchical ZSM-5 material so that the microporous and mesoporous material is formed in one structure. This results is different from the typical curve for microporous ZSM-5 isotherms which usually shows that specific surface area is developed from micropores [27], but it is consistent with the curve reported by Xu et al. [26] for hierarchical zeolites containing micro- and mesopores in one structure. In addition, the average diameter of the pores formed were 1.8842 nm and 2.7419 nm, which are within the range for microporous (d < 2 nm) and mesoporous (2 nm < d < 50 nm), respectively. The results for the surface area analysis are summarized in Table 1.

Table 1. Surface area and pore size hierarchical ZSM-5 with Mn_3O_4/ZSM-5.

Samples	S BET [a] (m^2/g)	S Micro [b] (m^2/g)	S Meso [c] (m^2/g)	Total Pore Volume [d] (cm^3/g)	Micropore Volume [e] (cm^3/g)	Mesoporous Volume [f] (cm^3/g)	Average Pore Diameter [g] (nm)	
							Micro-	Meso-
ZSM-5	348.6	199.1	149.5	0.2671	0.0969	0.17025	1.8842	2.7419
Mn_3O_4/ZSM-5	296.1	143.5	152.6	0.2467	0.0704	0.17626	1.8881	2.3979

[a.] BET method, [b.] T-plot analysis, [c.] a-b, [d.] the total pore volume at P / Po = 0.99, [e.] T-plot micropore volume, [f.] total volume—micropore volume, [g.] BJH method of desorption

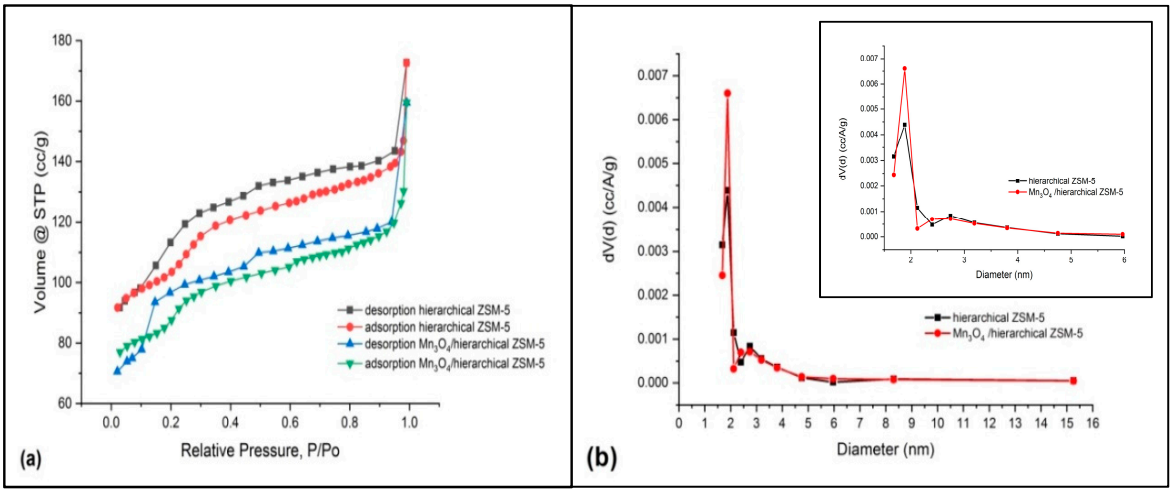

Figure 5. Comparison of; (**a**) isotherm adsorption-desorption graphs and (**b**) pore size distribution of ZSM-5 and Mn_3O_4/ZSM-5.

2.2. Cellulose Conversion Process Reaction of Delignified Rice Husk Waste to Levulinic Acid

2.2.1. Pre-Treatment of Rice Husk Waste

The first stage in the pre-treatment process for rice husk is dewaxing to remove extractive substances contained in the biomass such as wax, fat, fatty acids, terpenes, and steroids [28] that may interfere with the conversion process. The second stage is the delignification process to improve the internal surface of lignocellulose, reduce the degree of polymerization and crystallinity, and damage the structure of lignin [29]. Table 2 shows that before pre-treatment, the lignin and α-cellulose content were 33.53% and 42.37% weight, respectively. After pre-treatment, the lignin content decreased almost 49% to 17.24% weight in Table 2. The α-cellulose and hemicellulose content was also decreased. This may be due to cellulose and hemicellulose removal during the delignification process, especially the

part directly connected to lignin in the lignocellulosic bond [30]. The delignified rice husk is then used as a substrate in the catalytic test.

Table 2. Results for the chemical analysis of rice husk before and after treatment.

No.	Chemical Compounds	Yield (wt %)	
		Before Treatment	After Treatment
1	Lignin	33.53	17.24
2	α-Cellulose	42.37	25.66
3	Hemicellulose	10.70	5.75

2.2.2. Catalytic Test

The conversion of delignified cellulose to levulinic acid was conducted on three different types of Mn catalysts, i.e., Mn_3O_4/hierarchical ZSM-5 and solid Mn_3O_4 (heterogeneous catalysts), and Mn^{2+} solution (homogeneous catalyst). The Mn_3O_4 represent the Fenton-like species because it consists of Mn^{2+} and Mn^{3+} in the same structure [31,32], which in the presence of H_2O_2 could undergo reaction as in Equations (1) and (2). Furthermore, the role of hierarchical ZSM-5 as support catalyst was also studied by observing the reaction profile when Mn_3O_4/ZSM-5 is used as a catalyst. The reaction using hierarchical ZSM-5 as catalyst has been discussed in significant detail in our other work [17]. Finally, reaction with a homogeneous solution of Mn^{2+} catalyst was used as comparison, and the reaction without catalyst as control. All the reactions were carried out in phosphoric acid (H_3PO_4) 40% (v/v) media with reflux, since cellulose is soluble in phosphoric acid (which is able to damage the intra- and inter-molecular hydrogen bonds in cellulose) but difficult to dissolve in water [33]. The Fenton-like species was used for the next step, with phosphoric acid as media and the Fenton-like reaction of manganese also giving H^+ to the increased acidic media. The cellulose can be degraded using a Fenton-like reagent such as H_2O_2 together with a catalyst, and by a phosphoric acid solution [33].

$$Mn^{2+} + H_2O_2 \rightarrow Mn^{3+} + OH^- + HO\bullet \quad (1)$$

$$Mn^{3+} + H_2O_2 \rightarrow Mn^{2+} + HO_2\bullet + H^+ \quad (2)$$

The next step was breaking the β-(1,4)-glycosidic bonds, after the hydrogen bond termination by the solvent. The termination step occurred through Fenton-like reaction. Hydrogen peroxide was used in the presence of Mn(III) to produce a radical hydroxyl, HO• (Equation (1)). Therefore, hydrogen peroxide (H_2O_2) acted as an initiating reagent. The Mn^{3+} produced then reacts continuously with the H_2O_2, which in the presence of excess H_2O_2 produces Mn^{2+} and hydroperoxide radical, HO_2• (Equation (2)). However, radical hydroperoxides are not as effective as hydroxyl radicals [31,34]. Thus, the quantity of H_2O_2 used should not be too high to achieve optimum results [35]. The key mechanistic feature of the Fenton-like reaction is the generation of OH• radicals [34].

Figure 6 shows the percentage yield (wt %) of the reactions of delignified rice-husk over a 10 h-reaction time at 100 °C for three catalysts and without catalyst as control. The trends for yield (wt %) of produced levulinic acid were similar for all three catalysts, it was produced only after 2 h and kept increasing up to 8 h before decreasing after 10 h. In the reaction without catalysts, levulinic acid was only observed after the reaction has progressed for 4 h. This suggests that there is an initiation time for the reduction of β-1-4-glucosidic bonds in the cellulose to smaller fraction such as glucose, followed by oxidation of the hydroxyl radicals in both manganese and acidic media to produce levulinic acid.

To study the effect of temperature on the yield (wt %), reactions were also conducted at 130 °C; the results are shown in Figure 7. The result follows a similar trend to those obtained at 100 °C, but the yield (wt %) of levulinic acid is higher for the same reaction time. A significant increase in yield (wt %)

was observed in the reaction using Mn_3O_4/hierarchical ZSM-5 as catalyst, while the increase of yield (wt %) from other catalysts was less obvious.

Figures 6 and 7 show that the highest yield (wt %) of levulinic acid for each reaction was reached after 8 h reaction time. When using Mn_3O_4/hierarchical ZSM-5 as catalyst, the yield (wt %) obtained at 100 °C and 130 °C was 27.60% and 39.75%, respectively. The reaction using Mn^{2+} gave yield of 17.69% (100 °C) and 19.34% (130 °C). When Mn_3O_4 catalyst, the highest yield (wt %) of levulinic acid was similar, reaching 14.02% (100 °C) and 15.93% (130 °C), respectively. After 10 h reaction, the yield (wt %) of levulinic acid, for all catalysts, decreased. It indicates that the levulinic acid could decompose or undergo futher reaction. Based on this information, it is suggested that the reaction is selective to cellulose. This result recommends that cellulose degradation reactions requires higher temperatures (130 °C) to lower the activation energy [33]. The high reaction temperature give resulted in larger amount of products in the liquid hydrolysates, due to accelerated sugar structure decomposition and increased the severity of the treatment [36]. Longer reaction times and higher temperatures improve the yield of products by increasing the rate of degradation, which shows the relationship between the concentration and the reaction time. However, we do not go higher than 130 °C because we want it to be more selective to cellulose and keep the energy consumption as low as possible. In this reaction the remaining lignin mixed with other solid percipitate (char), as also reported in [17]. The fate of lignin was not discussed further, since usually lignin conversion, with or without the presence of catalyst, takes place at temperature above 150 °C with high preassure [37].

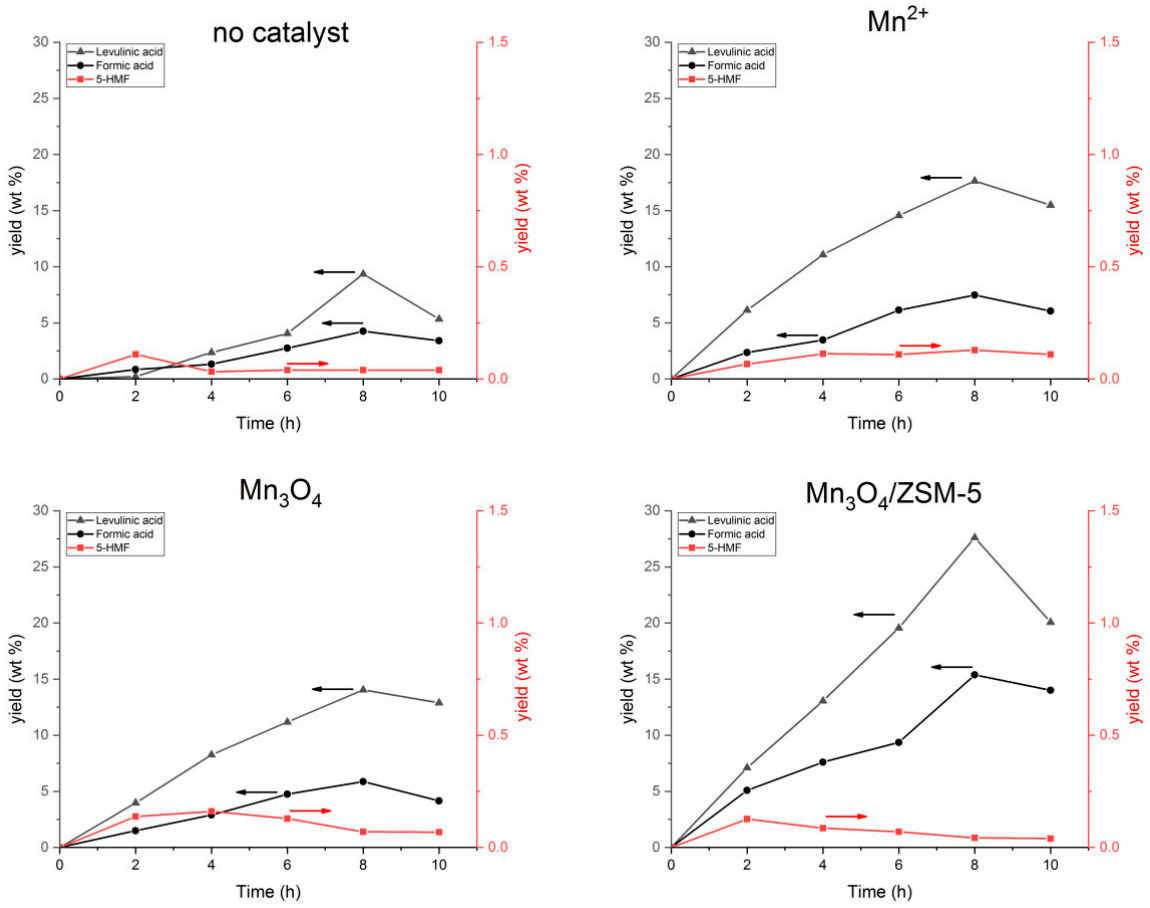

Figure 6. Percentage yield of 5-hydroxymethyl furfural (5 HMF) (**red**) levulinic acid, and formic acid (**black**) from the conversion reaction at 100 °C using different catalysts.

In the reaction using Mn^{2+}, Mn_3O_4, and hierarchical Mn_3O_4/ZSM-5 as catalysts, Mn species affected the formation of hydroxyl radicals that being generated during Fenton-like reaction. For the

reaction without a catalyst, there is no species to streamline the formation of hydroxyl radicals, hence, leading to a thermal decomposition of cellulose.

2.2.3. Side Product Analysis

Cellulose conversion, in acidic condition, to levulinic acid follows a complex reaction pathways [35], which involves the production of glucose, fructose, and 5-HMF as intermediates and formic acid as the by-product. In this work, only formation the of 5-HMF and formic acid were studied.

2.2.4. 5-HMF Intermediate

Figures 6 and 7 shows that the 5-HMF was not formed until 2 h of reaction, reached optimum 4 h, then decreased when the reaction carried out longer than 4 h. The decrease in 5-HMF yield indicates it has been converted futher into levulinic acid and formic acid. This trend is observed for all the manganese catalysts used in this study. In line with levulinic production, the reaction gives higher 5-HMF yield (wt %) at 130 °C than the reaction at 100 °C.

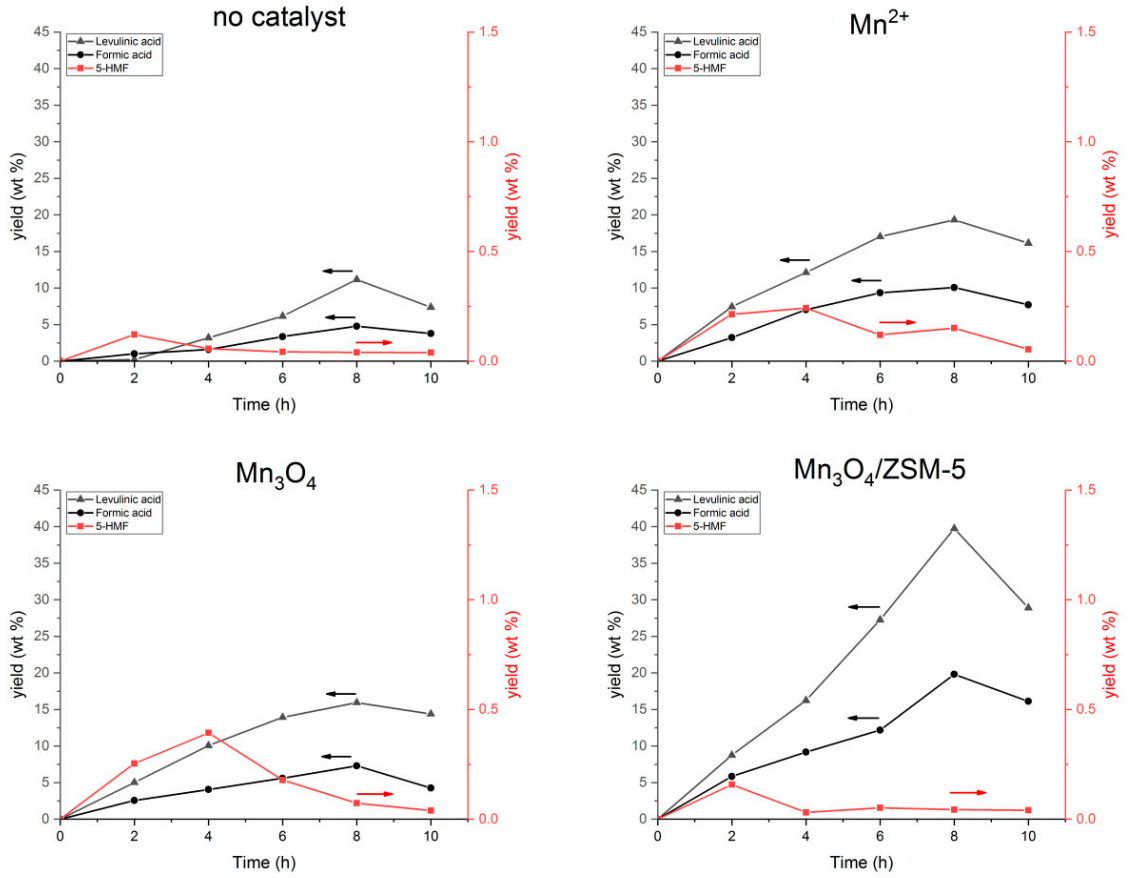

Figure 7. Percentage yield of 5 HMF (**red**) levulinic acid, and formic acid (**black**) from the conversion reaction at 130 °C using different catalysts.

2.2.5. Formic Acid

The results in Figures 6 and 7 show that formic acid is formed as a by-product because of two pathways from HMF intermediate compounds which produce levulinic acid as a main product and formic acid as a by-product [38]. The yield of formic acid follows the same trend as that of levulinic acid, which is the largest product obtained after 8 h of reaction. However, the yield of formic acid is lower than that of levulinic acid, due to evaporation at temperature above 100 °C.

3. Discussion

The presence of Mn catalysts has accelerated the process of delignified biomass conversion to levulinic acid. Comparing the activity of Mn^{2+} ion to solid Mn_3O_4, it was found that it is a better catalyst than the solid Mn_3O_4, giving a slightly higher yield (wt %) of levulinic acid. This is expected since in fenton like system, Mn^{2+} produced directly OH•, from H_2O_2, that will catalyze cellulose conversion to yield (wt %) of levulinic acid. Meanwhile, solid Mn_3O_4 is insoluble in water, hence, the amount of Mn^{2+} and Mn^{3+} produced will be less than that in the reaction using free Mn^{2+} catalyst. On the other hand, Mn_3O_4 impregnated to hierarchical ZSM-5 gives the highest % yield of levulinic acid among the three catalysts. It shows that, the ZSM-5, with high surface area, caused the Mn_3O_4 species distributed as small agregates inside the pores (as shown by TEM), thus it has more active sites than in bulk Mn_3O_4, producing more OH• species. This indicates that the hierarchical ZSM-5 plays an important role as a support catalyst. This result is consistent with our previous results [17] and results obtained by Chen et.al [33]. Unfortunately, the zeolite catalyst used in our reaction did not survive the acidic aqueous, as confirmed in our previous work [17]. This is a disadvantage using zeolite in severe aqueous phase reaction [39,40]. On the other hand, there are some advantages that can be gained in this reaction, such as small amount of catalyst used (10% of substrate weight), aqueous phase reaction, feasible separation of liquid product from unwanted solid char and lignin, less concentrated H_3PO_4 (40% v/v) and low reaction temperature (100 to 130 °C). They correspond to green chemistry and UN Sustainable Development Goals (SDGs) number 9 and 12 [41].

Analysis of the products is in agreement with the proposed mechanism for the production of levulinic acid from cellulose is illustrated in Figure 8. The cellulose from delignified rice husk first will be hydrolyzed to yield glucose, which is isomerized to form fructose. The fructose is then converted first to 5-HMF (intermediate product) and finally to levulinic acid, with formic acid as by-product [42]. Finally, a temperature of 130 °C give higher yield (wt %) results, since it speeds up the dehydration and rehydration processes from fructose to levulinic acid. The proposed mechanism is in agreement with mechanism reported by Chen et al. using cotton cellulose [33] and Singh et al. using aromatic crop [43].

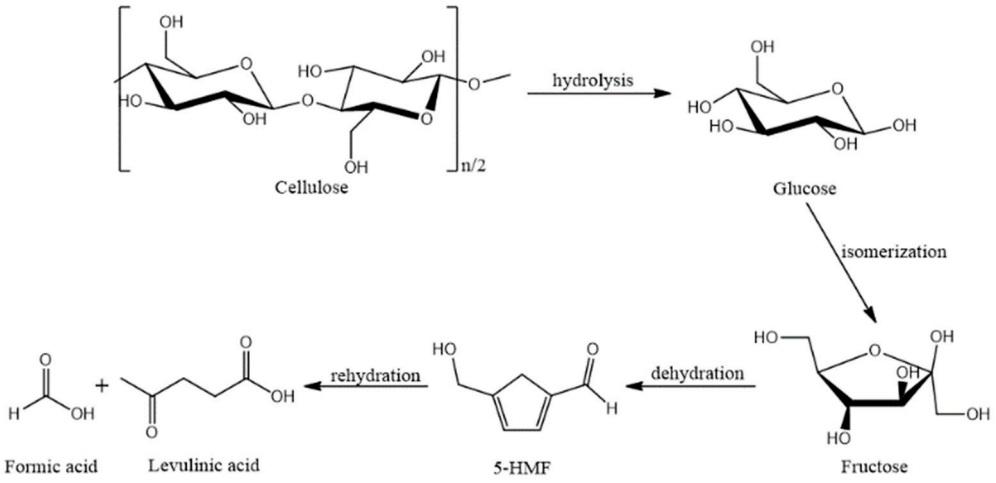

Figure 8. Proposed mechanism for cellulose conversion to yield levulinic acid.

4. Materials and Methods

4.1. Materials and Chemicals

Rice husk was supplied from Dramaga area, Bogor, Indonesia with the geographical coordinates -6.577672, 106.741376, harvested in dry season. The chemicals used in this experiment were all of analytical grade: hydrogen peroxide (30.0%, purity), phosphoric acid (89.0%, purity), sulphuric acid (96.0%, purity), sodium hydroxide (99.0%, purity), ethanol (95.0%, purity), and manganese (ii) nitrate

tetrahydrate (99.0%, purity) were obtained from Merck (Darmstadt, Germany) while tetraorthosilicate (TEOS, 98.0%), sodium aluminate (99.0%), tetrapropylammonium hydroxide (TPAOH, 1.0 M), and polidialydimethyl ammonium chloride (PDDA, 35.0%) were obtained from Sigma Aldrich (St. Louis, MO, USA). Distilled water was used in the preparation of each solution.

4.2. Preparation of Hierarchical ZSM-5 Zeolite, Hierarchical Mn_3O_4/ZSM-5 Zeolite, Mn_3O_4 and Mn(II) ion

The synthesis of hierarchical ZSM-5 zeolite was done following the procedure published in Krisnandi et al. [44], using a double template method with $NaAlO_2$ and TEOS as sources of Al and Si, and TPAOH and PDDA-Cl (35% wt) as first and second template sources. The crystallization process was carried out at 150 °C for 6 days. The product was filtered and calcined at 550 °C for 5 h to remove the organic template, followed by characterization using X-ray diffraction (XRD), Fourier transformed infra-red spectroscopy (FT-IR), Brunauer-Emmett-Teller (BET), and scanning electron microscopy-energy dispersive X-ray spectroscopy (SEM-EDS).

Hierarchical Mn_3O_4/ZSM-5 zeolite was prepared using the incipient wetness impregnation method with manganese nitrate solution for 24 h at 25 °C into a calcined hierarchical ZSM-5 zeolite. The mixture was dried at 110 °C for 5 h followed by calcination at 550 °C. For comparison, Mn_3O_4 and Mn(II) solutions were also prepared as catalysts. The Mn catalysts were then characterized accordingly using XRD, FTIR, BET, and atomic absorption spectroscopy (AAS).

XRD measurements of the samples were performed at the Physics Laboratory of BATAN PUSPIPTEK, Serpong, Indonesia. The crystal structures of the samples were measured at room temperature using XRD PANalytical Instrument with copper at λ Kα1 1.54096 Å. The X-ray source was a conventional sealed 2500-Watt X-ray tube operated at 45 kV and 40 mA in a 2θ range between 5° and 50°. The FT-IR sample measurements were performed using a Shimadzu IR Prestige 21. A mixture of dried solid sample and KBr was pelletized to form a transparent film for the measurement of the FT-IR at wavenumber range from 450 to 4000 cm^{-1}. SEM-EDS for analysis of the chemical composition at the Chemistry Laboratory, BATAN PUSPIPTEK, Serpong, Indonesia. The surface area and pore size were analysed using a Quantachrome Quadrawin v3.21 and ASAP 2400. Samples were measured by N_2 adsorption at 196 °C. The adsorption-desorption measurements for the samples were degassed at 300 °C for 13 h while the surface area was measured using the BET equation. The micropore and mesopore size distributions were determined using Barrett–Joyner–Halenda (BJH) methods. AAS was performed using a AA 6300. Destruction by digestion with nitric and perchloric acids and by low-temperature ashing with dissolution of the ash in a hydrofluoric acid mixture with solid sample. TEM measurement on ZSM-5 before and after Mn_3O_4 impregnation was carried out using Tecnai F20, FEI Company, KAIST.

4.3. Pre-Treatment of Biomass

Rice husk waste was subjected to dewaxing and delignification pre-treatment. Dewaxing was carried out by extracting the mash of the rice husk waste using *n*-hexane: ethanol (2:1, v/v) with soxhlet extraction for 6 h at 60 °C. Delignification was then carried out by immersing the residue from dewaxing process into 10% NaOH solution (1:25, m/v) at 55 °C for 90 min under vigorous stirring (200 rpm) The lignin and cellulose content were determined before and after the pre-treatment using the procedure outlined in our previous study [17].

4.4. Catalytic Test: Conversion of Delignified Rice Husk

The conversion of delignified rice husk (substrate) was carried out following Chen et al. [33] with modification. In general, it was conducted in Pyrex three neck-round bottom flask at 100 °C and 130 °C. Approximately 1 g of substrate was dispersed into 20 mL of phosphoric acid (40%, v/v) and 0.5 mL of hydrogen peroxide (30%, v/v). Hierarchical Mn_3O_4/ZSM-5 zeolite, Mn_3O_4, and Mn(II) ions were added in different amount as catalysts, adjusted to 10% of substrate weight. The mixture was heated at 100 or 130 °C, and sampled after 0, 2, 4, 6, 8, and 10 h reaction, quenched in ice-water bucket.

The liquid product was then separated from the precipitate and quantitatively measured using high performance liquid chromatography (HPLC), performed at the Department of Biology, UI using HPLC Ultimate 3000 on a silica gel column (RezexTM ROA-Organic Acid H^+ (8%)) equipped with a pump, autosampler, Rs column compartment, diode array detector UV at 210 nm for formic acid [45]; 220 nm for levulinic acid [17]; 284 nm for 5-HMF [33]. The eluent (H_2SO_4 0.0025 M) and distilled water were pumped at a flow rate of 1 mL/min.

4.5. Product Analysis

The yield (wt%) of products was calculated using the following Equation:

$$\%\ \text{yield of product} = \frac{\textit{total concentration}\ \left(\frac{mg}{L}\right) \times \textit{solution volume}\ (L)}{\textit{cellulose mass}\ (mg)} \times 100\% \quad (3)$$

5. Conclusions

The main role of hierarchical Mn_3O_4/ZSM-5 zeolite catalyst in this delignified rice husk conversion was its hierarchical porous ZSM-5 zeolite as porous material which accelerated the degradation of cellulose into levulinic acid. Mn oxide species also assisted in the Fenton-like reaction to form hydroxyl groups. The Mn_3O_4/ hierarchical ZSM-5 zeolite proved the best catalyst for the reaction, offering the highest percentage yield (wt %) of levulinic acid at 130 °C (39.75%) and 100 °C (27.60%) after 8 h as well as good selectivity toward levulinic acid than 5-HMF. It was also shown that the reaction temperature affects the yield (wt %) of levulinic acid.

Author Contributions: Conceptualization, Y.K.K.; formal analysis, A.P.P., D.U.C.R.; investigation, A.P.P.; writing—original draft preparation, A.P.P.; writing—review and editing, Y.K.K., D.U.C.R.; supervision, Y.K.K., and D.U.C.R.; project administration, Y.K.K.; funding acquisition, Y.K.K. All authors have read and agreed to the published version of the manuscript.

Funding: This work was funded by PUPT BPPTN 2018 grant No. 481/UN2.R3.1/HKP.05.00/2018 from Ministry of Research and Higher Education Republic of Indonesia.

Acknowledgments: Authors acknowledge the access for TEM and SEM measurement by Sung Min Choi and Aminah Umar from KAIST, and ENAGO proof reading with ASN Number: UNOINW-4221 for substantive editing service.

Conflicts of Interest: The authors declare no conflict of interest. The funders had no role in the design of the study; in the collection, analyses, or interpretation of data; in the writing of the manuscript, or in the decision to publish the results.

References

1. Girisuta, B.; Janssen, L.P.B.M.; Heeres, H.J. Green chemicals: A kinetic study on the conversion of glucose to levulinic acid. *Chem. Eng. Res. Des.* **2006**, *84*, 339–349. [CrossRef]
2. Alonso, D.M.; Wettstein, S.G.; Dumesic, J.A. Gamma-valerolactone, a sustainable platform molecule derived from lignocellulosic biomass. *Green Chem.* **2013**, *15*, 584–595. [CrossRef]
3. Kon, K.; Onodera, W.; Shimizu, K.I. Selective hydrogenation of levulinic acid to valeric acid and valeric biofuels by a Pt/HMFI catalyst. *Catal. Sci. Technol.* **2014**, *4*, 3227–3234. [CrossRef]
4. Burton, A. Recent trends in the synthesis of high-silica zeolites. *Catal. Rev. Sci. Eng.* **2018**, *60*, 132–175. [CrossRef]
5. Na, K.; Somorjai, G.A. Hierarchically Nanoporous Zeolites and Their Heterogeneous Catalysis: Current Status and Future Perspectives. *Catal. Lett.* **2015**, *145*, 193–213. [CrossRef]
6. Přech, J.; Pizarro, P.; Serrano, D.P.; Áejka, J. From 3D to 2D zeolite catalytic materials. *Chem. Soc. Rev.* **2018**, *47*, 8263–8306. [CrossRef]
7. Wang, L.; Zhang, Z.; Yin, C.; Shan, Z.; Xiao, F. Microporous and Mesoporous Materials Hierarchical mesoporous zeolites with controllable mesoporosity templated from cationic polymers. *Microporous Mesoporous Mater.* **2010**, *131*, 58–67. [CrossRef]

8. Inayat, A.; Knoke, I.; Spiecker, E.; Schwieger, W. Assemblies of mesoporous FAU-type zeolite nanosheets. *Angew. Chemie Int. Ed.* **2012**, *51*, 1962–1965. [CrossRef] [PubMed]
9. Shi, J.; Zhao, G.; Teng, J.; Wang, Y.; Xie, Z. Morphology control of ZSM-5 zeolites and their application in Cracking reaction of C4 olefin. *Inorg. Chem. Front.* **2018**, *5*, 2734–2738. [CrossRef]
10. Weckhuysen, B.M.; Yu, J. Recent advances in zeolite chemistry and catalysis. *Chem. Soc. Rev.* **2015**, *44*, 7022–7024. [CrossRef]
11. Krisnandi, Y.K.; Putra, B.A.P.; Bahtiar, M.; Zahara; Abdullah, I.; Howe, R.F. Partial Oxidation of Methane to Methanol over Heterogeneous Catalyst Co/ZSM-5. *Procedia Chem.* **2015**, *14*, 508–515. [CrossRef]
12. Yang, H.; Zhang, C.; Gao, P.; Wang, H.; Li, X.; Zhong, L.; Wei, W.; Sun, Y. A review of the catalytic hydrogenation of carbon dioxide into value-added hydrocarbons. *Catal. Sci. Technol.* **2017**, *7*, 4580–4598. [CrossRef]
13. Chen, H.; Shi, X.; Zhou, F.; Ma, H.; Qiao, K.; Lu, X.; Fu, J.; Huang, H. Catalytic fast pyrolysis of cellulose to aromatics over hierarchical nanocrystalline ZSM-5 zeolites prepared using sucrose as a template. *Catal. Commun.* **2018**, *110*, 102–105. [CrossRef]
14. Antonetti, C.; Galletti, A.M.R.; De Luise, V.; Licursi, D.; Nasso, N. Levulinic Acid Production from waste biomass. *J. Natl. Cancer Inst. Monogr.* **2014**, *7*, 1824–1835.
15. Kumar, P.; Barrett, D.M.; Delwiche, M.J.; Stroeve, P.; Kumar, P.; Barrett, D.M.; Delwiche, M.J.; Stroeve, P. Methods for Pretreatment of Lignocellulosic Biomass for Efficient Hydrolysis and Biofuel Production. *Ind. Eng. Chem. Res.* **2009**, *48*, 3713–3729. [CrossRef]
16. Rahayu, D.U.C.; Nurani, D.A.; Rochmah, L.N.H.; Antra, N.F.; Krisnandi, Y.K. A hierarchical MnOx/ZSM-5 heterogeneous catalyst for the conversion of cellulose from mahogany wood to levulinic acid. *IOP Conf. Ser. Mater. Sci. Eng.* **2019**, *496*, 012055. [CrossRef]
17. Krisnandi, Y.K.; Nurani, D.A.; Agnes, A.; Pertiwi, R.; Antra, N.F.; Anggraini, A.R.; Azaria, A.P.; Howe, R.F. Hierarchical MnOx/ZSM-5 as Heterogeneous Catalysts in Conversion of Delignified Rice Husk to Levulinic Acid. *Indones. J. Chem* **2019**, *19*, 115–123. [CrossRef]
18. Garcés, D.; Faba, L.; Díaz, E.; Ordóñez, S. Aqueous-Phase Transformation of Glucose into Hydroxymethylfurfural and Levulinic Acid by Combining Homogeneous and Heterogeneous Catalysis. *ChemSusChem* **2019**, *12*, 924–934.
19. Treacy, M.M.; Higgins, J.B. *Collection of Simulated XRD Powder Patterns for Zeolites*; Elsevier: Amsterdam, The Netherlands, 2001.
20. Wang, L.; Chen, L.; Li, Y.; Ji, H.; Yang, G. Preparation of Mn3O4 nanoparticles at room condition for supercapacitor application. *Powder Technol.* **2013**, *235*, 76–81. [CrossRef]
21. Pang, H.; Abdalla, A.M.; Sahu, R.P.; Duan, Y.; Puri, I.K. Low-temperature synthesis of manganese oxide–carbon nanotube-enhanced microwave-absorbing nanocomposites. *J. Mater. Sci.* **2018**, *53*, 16288–16302. [CrossRef]
22. Silverstein, R.M.; Webster, F.X.; Kiemle, D.J. *Spectrometric Identification of Organic Compounds*; John Wiley & Sons: Hoboken, NJ, USA, 2005; ISBN 0-471-39362-2.
23. Tian, Z.Y.; Mountapmbeme Kouotou, P.; Bahlawane, N.; Tchoua Ngamou, P.H. Synthesis of the catalytically active Mn3O4 spinel and its thermal properties. *J. Phys. Chem. C* **2013**, *117*, 6218–6224. [CrossRef]
24. Wang, Y.; Zhu, L.; Yang, X.; Shao, E.; Deng, X.; Liu, N.; Wu, M. Facile synthesis of three-dimensional Mn 3 O 4 hierarchical microstructures and their application in the degradation of methylene blue. *J. Mater. Chem. A* **2015**, *3*, 2934–2941. [CrossRef]
25. Zhang, J.; Li, X.; Liu, J.; Wang, C. A Comparative Study of MFI Zeolite Derived from Different Silica Sources: Synthesis, Characterization and Catalytic Performance. *Catalysts* **2018**, *9*, 13. [CrossRef]
26. Xu, L.; Wang, F.; Feng, Z.; Liu, Z.; Guan, J. Hierarchical ZSM-5 Zeolite with Enhanced Catalytic Activity for Alkylation of Phenol with Tert-Butanol. *Catalysts* **2019**, *9*, 202. [CrossRef]
27. Al-Thawabeia, R.A.; Hodali, H.A. Use of Zeolite ZSM-5 for Loading and Release of 5-Fluorouracil. *J. Chem.* **2015**, *2015*, 1–9. [CrossRef]
28. Basu, P. *Biomass Gasification and Pyrolysis*; Elsevier: Oxford, UK, 2010; ISBN 978-0-12-374988-8.
29. Zhao, X.; Zhang, L.; Liu, D. Biomass recalcitrance. Part II: Fundamentals of different pre-treatments to increase the enzymatic digestibility of lignocellulose. *Biofuels Bioprod. Biorefining* **2012**, *6*, 561–579. [CrossRef]
30. Kumar, A.K.; Sharma, S. Recent updates on different methods of pretreatment of lignocellulosic feedstocks: A review. *Bioresour. Bioprocess.* **2017**, *4*, 7. [CrossRef]

31. Rhadfi, T.; Piquemal, J.Y.; Sicard, L.; Herbst, F.; Briot, E.; Benedetti, M.; Atlamsani, A. Polyol-made Mn3O4 nanocrystals as efficient Fenton-like catalysts. *Appl. Catal. A Gen.* **2010**, *386*, 132–139. [CrossRef]
32. Azadmanesh, J.; Borgstahl, G. A Review of the Catalytic Mechanism of Human Manganese Superoxide Dismutase. *Antioxidants* **2018**, *7*, 25. [CrossRef]
33. Chen, Y.; Li, G.; Yang, F.; Zhang, S. Mn/ZSM-5 participation in the degradation of cellulose under phosphoric acid media. *Polym. Degrad. Stab.* **2011**, *96*, 863–869. [CrossRef]
34. Dhakshinamoorthy, A.; Navalon, S.; Alvaro, M.; Garcia, H. Metal nanoparticles as heterogeneous fenton catalysts. *ChemSusChem* **2012**, *5*, 46–64. [CrossRef] [PubMed]
35. Gardner, D.W.; Huo, J.; Hoff, T.C.; Johnson, R.L.; Shanks, B.H.; Tessonnier, J.P. Insights into the Hydrothermal Stability of ZSM-5 under Relevant Biomass Conversion Reaction Conditions. *ACS Catal.* **2015**, *5*, 4418–4422. [CrossRef]
36. Jeong, H.; Park, S.; Ryu, G.; Choi, J.; Kim, J.; Choi, W. Catalytic conversion of hemicellulosic sugars derived from biomass to levulinic acid. *Catal. Commun.* **2018**, *117*, 19–25. [CrossRef]
37. Otromke, M.; White, R.J.; Sauer, J. Hydrothermal base catalyzed depolymerization and conversion of technical lignin—An introductory review. *Carbon Resour. Convers.* **2019**, *2*, 59–71. [CrossRef]
38. Qi, Y.; Song, B.; Qi, Y. The roles of formic acid and levulinic acid on the formation and growth of carbonaceous spheres by hydrothermal carbonization. *RSC Adv.* **2016**, *6*, 102428–102435. [CrossRef]
39. Prodinger, S.; Shi, H.; Eckstein, S.; Hu, J.Z.; Olarte, M.V.; Camaioni, D.M.; Derewinski, M.A.; Lercher, J.A. Stability of Zeolites in Aqueous Phase Reactions. *Chem. Mater.* **2017**, *29*, 7255–7262. [CrossRef]
40. Ravenelle, R.M.; Schübler, F.; Damico, A.; Danilina, N.; Van Bokhoven, J.A.; Lercher, J.A.; Jones, C.W.; Sievers, C. Stability of zeolites in hot liquid water. *J. Phys. Chem. C* **2010**, *114*, 19582–19595. [CrossRef]
41. Poliakoff, M.; Licence, P.; George, M.W. UN sustainable development goals: How can sustainable/green chemistry contribute? By doing things differently. *Curr. Opin. Green Sustain. Chem.* **2018**, *13*, 146–149. [CrossRef]
42. Weingarten, R.; Conner, W.C.; Huber, G.W. Production of levulinic acid from cellulose by hydrothermal decomposition combined with aqueous phase dehydration with a solid acid catalyst. *Energy Environ. Sci.* **2012**, *5*, 7559–7574. [CrossRef]
43. Singh, M.; Pandey, N.; Dwivedi, P.; Kumar, V.; Mishra, B.B. Production of xylose, levulinic acid, and lignin from spent aromatic biomass with a recyclable BrØnsted acid synthesized from d-limonene as renewable feedstock from citrus waste. *Bioresour. Technol.* **2019**, *293*, 122105. [CrossRef]
44. Krisnandi, Y.K.; Nurani, D.A. Akmal Partial Oxidation of Methane Over NiOx / Hierachichal ZSM-5 Catalyst Partial Oxidation of Methane Over NiOx / Hierachichal ZSM-5 Catalyst. *IOP Conf. Ser. J. Phys. Conf. Ser.* **2018**, *1095*, 012005.
45. Minnaar, P.P.; Swan, G.E.; McCrindle, R.I.; De Beer, W.H.J.; Naudé, T.W. A high-performance liquid chromatographic method for the determination of monofluoroacetate. *J. Chromatogr. Sci.* **2000**, *38*, 16–20. [CrossRef] [PubMed]